Springer

KSME

Journal of Mechanical Science and Technology 30 (3) (2016) 1077~1084
www.springerlink.com/content/1738-494x(Print)/1976-3824(Online)
DOI 10.1007/s12206-016-0212-8

Springback prediction of the vee bending process for high-strength steel sheets †

Daw-Kwei Leu* and Zhi-Wei Zhuang

Department of Mechanical Engineering, Taipei Chengshih University of Science and Technology, No. 2, Xueyuan Road, Beitou, Taipei 112, Taiwan, Republic of China

(Manuscript Received November 19, 2014; Revised July 27, 2015; Accepted November 3, 2015)

Abstract

The precise prediction of springback is a key to assessing the accuracy of part geometry in sheet bending. A simplified approach is developed by considering the thickness ratio, normal anisotropy, and the strain-hardening exponent to estimate the springback of vee bending based on elementary bending theory. Accordingly, a series of experiments is performed to verify the numerical simulation. The calculation of the springback angle agrees well with the experiment, which reflects the reliability of the proposed model. The effects of process parameters such as punch radius, material strength, and sheet thickness on the springback angle are experimentally tested to determine the dominant parameters for reducing the springback angle in the sheet bending process for high-strength steel sheets. Moreover, the effects of the thickness ratio, normal anisotropy, and the strain-hardening exponent on the springback angle in the vee bending process for high-strength steel sheets are theoretically studied. Therefore, improving understanding on and control of the springback reduction of the vee bending process in practical applications is possible.

Keywords: Sheet; Bending; Springback; Anisotropy; Hardening

1. Introduction

The bending processes of metal sheets are widely used to produce structural stamping parts. The most important metal sheet bending process is vee bending, which includes two subprocesses: air bending and coining. The understanding and development of bending mechanics aim to obtain the following techniques, which are important for practical applications: (i) springback prediction for tool design, process, and component shape accuracy control, and (ii) failure prediction (originating from the stretched surface) or bendability (the minimum bending radius) assessment. Elastic recovery after unloading causes the springback phenomenon in which the curvature radius of any bending fiber increases after bending moment is removed. The precise prediction of springback after bending unloading is the key to the tool design, process control, and accuracy assessment of part geometry.

Considerable efforts have been exerted to improve the understanding of this phenomenon. Gardiner [1] investigated the springback of metals. Datsko and Yang [2] demonstrated how the bendability of materials correlated with their tensile properties. Takenaka et al. [3] studied the material characteristic values for evaluating bendability and the methods for measuring these values. Cupka et al. [4] examined fine bending with counter pressure. Kals and Veenstra [5] explored critical radius in sheet bending. Accordingly, Ogawa et al. [6] developed an elastic plastic Finite element (FE) model for accurately predicting springback in the sheet bending process and validated this model through experiments. Wang et al. [7] built a mathematical model of the plane strain bending of metal sheets. Leu [8] established a simplified approach for evaluating bendability and springback in the bending of anisotropic metal sheets. Leu [9] studied the effects of process parameters on the vee bending process for steel sheets using the FE method. Huang [10] investigated the coining process of vee bending using an elastic plastic FE method. Recently, Leu and Hsieh [11] analyzed how coining force would affect springback reduction in the vee bending process. Bakhshi-Jooybari et al. [12] experimentally and theoretically examined the effects of significant parameters on the springback in the U-bending and V-bending of CK67 anisotropic steel sheets. Narayanasamy and Padmanabhan [13] explored the application of response surface methodology to predict bending force during the air-bending process. Yu [14] evaluated the variation of elastic modulus during plastic deformation and its influence on springback. Ozturk et al. [15] concluded that warm temperature was an offset in springback increase for titanium sheets. Chatti and Hermi [16] examined springback prediction based on nonlinear recovery. Baseri et al. [17] developed a springback model of the vee bending process using the back-propagation algorithm of fuzzy learning. Chen and Jiang [18]

*Corresponding author. Tel.: +886 2 2892 7154 ext.8012
E-mail address: dkleu@tpcu.edu.tw
† Recommended by Associate Editor Choon Yeol Lee

determined how grain size would affect the micro V-bending process for thin sheet metals. Lee et al. [19] studied how anisotropic hardening would influence springback prediction in prestrained U-draw/bending. Jiang and Chen [20] researched how grain size would affect springback behavior in micro tube-bending. Fu [21] analyzed the influencing factors of springback for air bending using the ABAQUS FEA software. Malikov et al. [22] experimentally and theoretically investigated bending force for the air bending of structured metal sheets. Song and Yu [23] studied the springback prediction of bending for a T-section beam using an FE method associated with a neural network technique. Recently, a pioneer work on a new topic concerning the position deviation of bending point in symmetric vee bending with an asymmetric bent length was conducted by Leu [24].

Given its high strength and low cost compared with conventional metals, High-strength steel (HSS) is widely used in automotive body structures, particularly, to reduce weight, which consequently reduces energy use. Weinmann and Shippell [25] discussed the effects of tool and workpiece geometries on the bending forces and springback in the vee bending of high-strength low-alloy steel sheets. Ramezani et al. [26] used the Stribeck friction model to investigate the springback behavior of HSS sheets using the FE method in the V-bending process. Fu and Mo [27] numerically examined the incremental air-bending process for high-strength metal sheets. Ramezani and Mohd Ripin [28] proposed a dry friction model, which was a function of the strain-hardening exponent and the contact area ratio, to explore the vee bending process of aluminum alloy 6061-T4 sheets using ABAQUS/Standard. Fu and Mo [29] studied springback prediction and tool design in air bending for high-strength metal sheets based on the genetic algorithm-backpropagation neural network technique. Kardes Sever et al. [30] analyzed the effect of the *E*-modulus that was varied with strain on springback prediction in the V-bending and U-bending of advanced HSS (AHSS-DP 780). Recently, Leu [31] conducted a preliminary study on the position deviation of the bending point for the V-die bending process with asymmetric dies to examine the amount of deviation and the position of the bending point for HSS sheets SPFC 440 and 590 of JIS G3135. Although considerable progress has been achieved to improve the modeling of sheet bending, further advancement of existing theories is required to enable practical applications of these findings.

Metal sheets, which are mostly manufactured by rolling processes, have mechanical properties that vary with rolling direction as a result of either preferred crystallographic orientation or mechanical fibering. This is known as anisotropy, which should be considered for a more realistic modeling of sheet metal bending. In the present study, normal anisotropy and strain hardening are incorporated to consider their effects on springback prediction.

The springback phenomenon in bending typically accounts for a large amount of setup time. Therefore, a simple method for computing springback is valuable for practical applications. In the present study, material characteristics (nonlinear strain hardening and normal anisotropy) and tool geometry under the plane strain condition of pure bending are integrated into the model. A simplified equation for predicting the springback angle is developed based on elementary bending theory of plasticity. The proposed model is different from other works, which consider the high-order term (a quadric term) of bending strain to obtain a precise evaluation of springback within the region of nonlinear plastic deformation. Moreover, a series of experiments is performed to verify the present model. The proposed model can be used as a guideline for tool and product design.

2. Analysis

To reduce the complexities involved in the analysis, the following simplified assumptions are made.

(1) A rigid plastic, strain-hardening, and anisotropic material is assumed to exhibit bending behavior in the region of plastic deformation.

(2) Bending deformation is expected to occur under the plane strain condition to simplify the analyzed model.

(3) The Bauschinger effect and the strain rate are neglected to remain consistent in the deformation behavior between tension and compression.

(4) Hill's theory of plastic anisotropy is used to describe the normal anisotropic characteristics of metal sheets.

The normal anisotropic value is a mechanical property of the metal sheet material, which is generally defined as

$$R = \frac{R_0 + 2R_{45} + R_{90}}{4}, \tag{1}$$

where R_0, R_{45} and R_{90} denote the anisotropic values measured at 0°, 45° and 90° of rolling direction, respectively.

The strain-hardening characteristics of the sheet are expressed as

$$\sigma_e = K(\varepsilon_0 + \varepsilon_p)^n, \tag{2}$$

where σ_e denotes effective stress, ε_p indicates effective strain, and K represents a material constant. The power law equation can be derived using a simple tensile test in which the initial strain is $\varepsilon_0 = (\sigma_y / K)^{1/n}$ and σ_y is the yield strength of the metal sheet.

A schematic diagram of the vee bending process is provided in Fig. 1, and the pure bending model shown in Fig. 2 is used to develop the springback model of vee bending.

2.1 Pure bending moment M

In the bending model shown in Fig. 2, the applied bending moment of pure bending, which is based on elementary bending theory, is

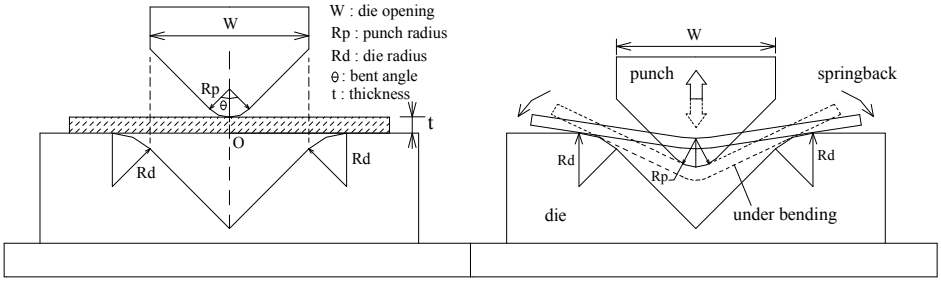

(a) (b)

Fig. 1. (a) Vee bending process; (b) springback after unloading.

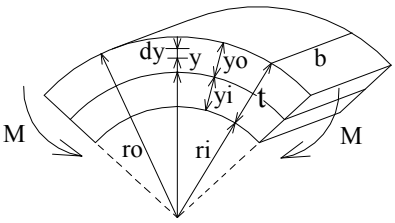

Fig. 2. Pure bending model.

$$M = 2b\int_0^{\frac{t}{2}} \sigma_\theta y dy\,, \tag{3}$$

where σ_θ is the circumferential stress, and

$$\sigma_\theta = \frac{1+R}{\sqrt{1+2R}}\sigma_e \quad \text{and} \quad \varepsilon_\theta = \frac{\sqrt{1+2R}}{1+R}\varepsilon_p\,, \tag{4}$$

which obey Hill's theory of plastic anisotropy. ε_θ is the circumferential strain, and R is the measure of normal anisotropy. Accordingly, the circumferential strain ε_θ can be expressed as

$$\varepsilon_\theta = \ln\left[\frac{\rho+y}{\rho}\right]. \tag{5}$$

Considering the quadric term of the series for the natural logarithm function, the circumferential strain can be reduced to two terms, *i.e.,* the linear term and the quadric term,

$$\varepsilon_\theta = \ln\left(1+\frac{y}{\rho}\right) \approx \left[\frac{y}{\rho} - \frac{1}{2}\left(\frac{y}{\rho}\right)^2\right]. \tag{6}$$

The circumferential strain shown in Eq. (6) is more precise than that in $\varepsilon_\theta \approx y/\rho$ (the linear term only). The present model considers both the linear term and the quadric term in circumferential strain. Circumferential stress σ_θ can then be expressed as

$$\begin{aligned}\sigma_\theta &= \frac{1+R}{\sqrt{1+2R}}\sigma_e = \frac{1+R}{\sqrt{1+2R}}K\left(\varepsilon_0+\varepsilon_p\right)^n \\ &= \frac{1+R}{\sqrt{1+2R}}K\left(\varepsilon_0 + \frac{1+R}{\sqrt{1+2R}}\varepsilon_\theta\right)^n \\ &\approx K\frac{1+R}{\sqrt{1+2R}}\left\{\varepsilon_0 + \frac{1+R}{\sqrt{1+2R}}\left[\frac{y}{\rho} - \frac{1}{2}\left(\frac{y}{\rho}\right)^2\right]\right\}^n\end{aligned}. \tag{7}$$

Furthermore, a simplified form of the series, $\left(a_0+b_0\right)^m \cong a_0^m + ma_0^{m-1}b_0$ ($a_0^2 > b_0^2$), is used to simplify Eq. (7) to develop the bending model. Eq. (7) can then be rewritten as

$$\begin{aligned}\sigma_\theta &= K\frac{1+R}{\sqrt{1+2R}}\left\{\frac{1+R}{\sqrt{1+2R}}\left[\frac{y}{\rho} - \frac{1}{2}\left(\frac{y}{\rho}\right)^2\right] + \varepsilon_0\right\}^n \\ &= K\frac{1+R}{\sqrt{1+2R}}\left(a_0+b_0\right)^m \quad ; \quad \text{(8a)} \\ &\approx K\frac{1+R}{\sqrt{1+2R}}\left\{\begin{array}{l}\left(\frac{1+R}{\sqrt{1+2R}}\right)^n\left[\frac{y}{\rho} - \frac{1}{2}\left(\frac{y}{\rho}\right)^2\right]^n + n\varepsilon_0 \\ \left(\frac{1+R}{\sqrt{1+2R}}\right)^{n-1}\left[\frac{y}{\rho} - \frac{1}{2}\left(\frac{y}{\rho}\right)^2\right]^{n-1}\end{array}\right\}\end{aligned}$$

then

$$\sigma_\theta \approx K\frac{1+R}{\sqrt{1+2R}}\left\{\begin{array}{l}\left(\frac{1+R}{\sqrt{1+2R}}\right)^n\left[\left(\frac{y}{\rho}\right)^n - \frac{n}{2}\left(\frac{y}{\rho}\right)^{n+1}\right] + \\ n\varepsilon_0\left(\frac{1+R}{\sqrt{1+2R}}\right)^{n-1}\left[\left(\frac{y}{\rho}\right)^{n-1} - \frac{(n-1)}{2}\left(\frac{y}{\rho}\right)^n\right]\end{array}\right\}. \tag{8b}$$

By substituting Eq. (8b) into Eq. (3), the applied bending moment of pure bending can be expressed as

$$M = 2b\int_0^{\frac{t}{2}} \overline{\overline{C}}\left[C\left(\frac{y}{\rho}\right)^{n-1} + A\left(\frac{y}{\rho}\right)^{n} + B\left(\frac{y}{\rho}\right)^{n+1}\right] y dy$$
$$= \frac{b\overline{\overline{C}}}{2}t^2\left[\begin{array}{l}\dfrac{C}{n+1}\left(\dfrac{t}{2\rho}\right)^{n-1} + \dfrac{A}{n+2}\left(\dfrac{t}{2\rho}\right)^{n} \\ + \dfrac{B}{n+3}\left(\dfrac{t}{2\rho}\right)^{n+1}\end{array}\right], \quad (9)$$

where A, B, C, $\overline{C}$ and $\overline{\overline{C}}$ are constant.

$$A = \overline{C}^{n} - \frac{n(n-1)}{2}\varepsilon_0\overline{C}^{n-1} = \left(\frac{1+R}{\sqrt{1+2R}}\right)^{n} - \frac{n(n-1)}{2}\varepsilon_0\left(\frac{1+R}{\sqrt{1+2R}}\right)^{n-1} \quad (10)$$

$$B = -\frac{n}{2}\overline{C}^{n} = -\frac{n}{2}\left(\frac{1+R}{\sqrt{1+2R}}\right)^{n} \quad (11)$$

$$C = n\varepsilon_0\overline{C}^{n-1} = n\varepsilon_0\left(\frac{1+R}{\sqrt{1+2R}}\right)^{n-1} \quad (12)$$

$$\overline{C} = \frac{1+R}{\sqrt{1+2R}} \quad (13)$$

$$\overline{\overline{C}} = K\overline{C} = K\frac{1+R}{\sqrt{1+2R}}. \quad (14)$$

Eq. (9) shows the applied bending moment, which is a function of tool geometry and material properties.

2.2 Springback ratio $\Delta\theta/\theta$

Elastic recovery after unloading causes the springback phenomenon. Precisely predicting springback is a key to assessing the accuracy of part geometry. The unloading moment ΔM is assumed to have the same magnitude but opposite sign as the applied bending moment M, *i.e.*, $\Delta M = -M$. The form of elastic deformation is

$$\Delta\sigma_\theta = -\frac{My}{I} = E'\Delta\varepsilon_\theta \text{ and } E' = \frac{E}{(1-\nu^2)}, \quad (15)$$

under the plane strain condition. Then,

$$\Delta\varepsilon_\theta = \frac{\Delta\sigma_\theta}{E'} = -\frac{My}{E'I} \text{ and } \Delta\varepsilon_\theta = y\left(\frac{1}{\rho^*} - \frac{1}{\rho}\right). \quad (16)$$

From Eq. (16), the following relationship is obtained:

$$\frac{1}{\rho^*} = \frac{1}{\rho} - \frac{M}{E'I}, \quad (17)$$

where ρ and ρ^* are the radii of the neutral axes before and after unloading, respectively.

Under the elastic unloading of elementary bending theory, the unloading moment ΔM is

$$\Delta M = -M = \frac{bEt^3}{12(1-\nu^2)}\left(\frac{1}{\rho} - \frac{1}{\rho^*}\right). \quad (18)$$

As unloading occurs, the springback angle is

$$\Delta\theta = \theta - \theta^*. \quad (19)$$

During its conversion to a dimensionless unit, the springback ratio is defined as

$$\frac{\Delta\theta}{\theta} = 1 - \frac{\theta^*}{\theta} = 1 - \frac{\rho}{\rho^*} = \frac{M}{E'I}\rho, \quad (20)$$

under the condition of $\rho\theta = \rho^*\theta^*$, *i.e.*, the arc length of the neutral axes is invariant before and after unloading.

By substituting Eq. (9) into the aforementioned equation, the springback ratio can then be expressed as

$$\frac{\Delta\theta}{\theta} = \frac{\rho}{E'I}\frac{b\overline{\overline{C}}}{2}t^2\left[\begin{array}{l}\dfrac{C}{n+1}\left(\dfrac{t}{2\rho}\right)^{n-1} + \dfrac{A}{n+2}\left(\dfrac{t}{2\rho}\right)^{n} \\ + \dfrac{B}{n+3}\left(\dfrac{t}{2\rho}\right)^{n+1}\end{array}\right]$$
$$= \frac{3}{E'}\overline{\overline{C}}\left[\begin{array}{l}\dfrac{C}{n+1}\left(\dfrac{t}{2\rho}\right)^{n-2} + \dfrac{A}{n+2}\left(\dfrac{t}{2\rho}\right)^{n-1} + \\ \dfrac{B}{n+3}\left(\dfrac{t}{2\rho}\right)^{n}\end{array}\right] \quad (21)$$

or

$$\left(\frac{\Delta\theta}{\theta}\right)\Big/\left(3\frac{K}{E'}\right) = \left[\frac{n\varepsilon_0}{n+1}\left(\frac{1+R}{\sqrt{1+2R}}\right)^{n}\left(\frac{t}{2\rho}\right)^{n-2} + \frac{1}{n+2}\left[\left(\frac{1+R}{\sqrt{1+2R}}\right)^{n+1} - \frac{n(n-1)}{2}\varepsilon_0\left(\frac{1+R}{\sqrt{1+2R}}\right)^{n}\right]\cdot \left(\frac{t}{2\rho}\right)^{n-1} - \frac{n}{2(n+3)}\left(\frac{t}{2\rho}\right)^{n}\left(\frac{1+R}{\sqrt{1+2R}}\right)^{n+1}\right] \quad (22)$$

Eq. (22) shows the springback ratio, which is a function of material properties (initial strain ε_0, the strain-hardening exponent n, and normal anisotropy R) and tool geometry (thickness ratio $t/2\rho$).

3. Results and discussion

Experimental measurements and numerical simulations were performed in this work. Experiments were conducted on the springback angle of bending for various process parame-

Table 1. Material properties of the HSS sheet manufactured by China Steel Company [24].

JIS G3135	t/mm	E/GPa	ν	σ_y/MPa	$\sigma = K(\varepsilon_0 + \varepsilon_p)^n$/MPa
SPFC 440	1.4	205	0.3	285.9	$\sigma = 745.9(0.00126 + \varepsilon_p)^{0.212}$
SPFC 440	1.8	205	0.3	313.9	$\sigma = 739.9(0.00153 + \varepsilon_p)^{0.201}$
SPFC 590	1.8	205	0.3	287.8	$\sigma = 1161.6(0.0014 + \varepsilon_p)^{0.257}$

Table 2. Tool dimensions and experimental results of vee bending.

$R_P = 6$ mm $R_d = 3$ mm	Thickness t/mm	Calculation $\Delta\theta_c$/°	Calculation $\Delta\theta_c^*$/°	Experiment $\Delta\theta_e$/°	Error A $\Delta\theta_c - \Delta\theta_e$	Error B $\Delta\theta_c^* - \Delta\theta_e$
SPFC 440	1.4	3.12	1.41	2.67	0.45	−1.26
SPFC 440	1.8	2.66	1.21	2.27	0.39	−1.06
SPFC 590	1.8	3.66	1.63	3.33	0.33	−1.70
$R_P = 3$ mm $R_d = 3$ mm	Thickness t/mm	Calculation $\Delta\theta_c$/°	Calculation $\Delta\theta_c^*$/°	Experiment $\Delta\theta_e$/°	Error A $\Delta\theta_c - \Delta\theta_e$	Error B $\Delta\theta_c^* - \Delta\theta_e$
SPFC 440	1.4	1.94	0.88	2.25	−0.31	−1.37
SPFC 440	1.8	1.51	0.77	2.23	−0.72	−1.46
SPFC 590	1.8	2.37	1.07	2.75	−0.38	−1.68

W = 25 mm shown in Fig. 1; lubricant: WD−40 mineral oil and $R = 1$; $\Delta\theta_c^*$ based on Eq. (23) in Ref. [8].

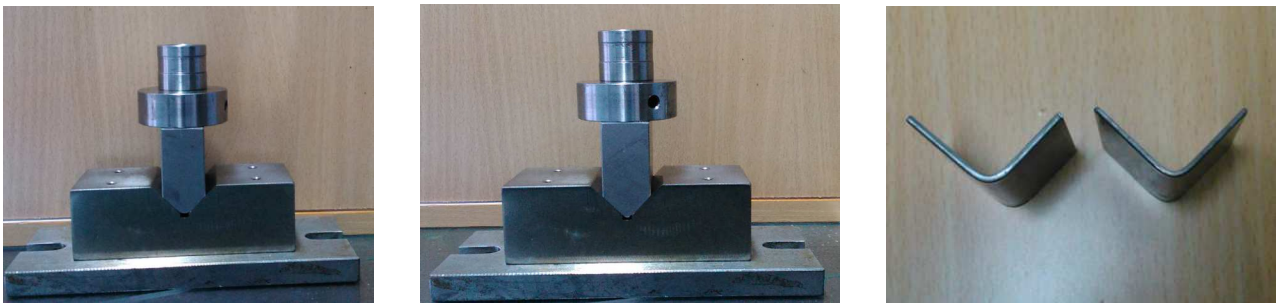

(a) $Rp = 6$ mm (b) $Rp = 3$ mm (c) Test workpiece

Fig. 3. Experimental tools for vee bending, W = 25 mm and $R_d = 3$ mm.

ters, such as punch radius, sheet thickness, and material strength. An experiment was performed to verify the efficiency of the developed model. A numerical simulation was also performed to investigate the effects of several process parameters on the springback ratio of the vee bending process using Eq. (22). The experimental materials were supplied by China Steel Corporation, as shown in Table 1 or in Ref. [24]. Figs. 1 and 3 show the schemes of the die, the punch head, and the bent shape of the test piece. The detailed dimensions of the tools for the experiments are listed in Table 2. A lubricant, namely, WD-40 mineral oil, was used in the experiments. Experiments were performed using a 300 kN hydraulic test machine, and optical equipment was used to measure the springback angle.

As shown in Eq. (22), the springback angle is directly proportional to initial strain ε_0 and inversely proportional to the modulus of elasticity E within an elastic limit. The modulus of elasticity E represents stiffness, which is an important mechanical property. A large ε_0 indicates a small E.

3.1 Verifying the springback angle $\Delta\theta$

The predicted results of the springback angle, which are calculated using Eq. (22), are compared with the experimental values. The predicted springback angles agree well with the experimental values presented in Table 2, where errors range from −0.72° to 0.45° in Error A ($\Delta\theta_c - \Delta\theta_e$). This result indicates the reliability of the present method. To verify the improvement of the present model, Eq. (23), which is derived in Ref. [8], is compared with Eq. (22).

$$\frac{\Delta\theta}{\theta} = \frac{UTS}{e^{-n}n^n}\left(\frac{1+R}{\sqrt{1+2R}}\right)^{1+n}\frac{3(1-\nu)^2}{2E(1+n)}\left(\frac{t}{2\rho}\right)^{n-1}, \tag{23}$$

in which UTS is the tensile strength of the material, and $UTS/(e^{-n}n^n)$ is equal to K.

The predicted results of the springback angle calculated using Eq. (23) are compared with the experimental measurements provided in Table 2. Table 2 shows that the predicted

springback angles calculated using Eq. (23) obviously disagree with the measurements, and errors range from −1.06° to 1.70° in Error B ($\Delta\theta_c^* - \Delta\theta_e$). This difference indicates the reliability of the present method and demonstrates that the present model is better than the model proposed by Leu in Ref. [8] for the springback prediction of HSS sheets.

3.2 Effects of material properties and tool geometry on the springback angle based on experiments

The effects of punch radius, sheet thickness, and material strength on the springback angle are shown in Figs. 4(a)-(c), respectively, based on the experimental results. Fig. 4(a) shows that the springback angle increases as sheet thickness decreases under SPFC 440, punch radius *Rp* = 6, and thickness *t* = 3 mm. This effect is attributed to considerable thickness, which reduces the influence of elastic sheet recovery because of the increase in bulk deformation. However, the increase in the springback angle is limited in the case of *Rp* = 3 mm. The result shows that punch radius plays an important role in springback occurrence. Fig. 4(b) illustrates that the springback angle increases as material strength increases (SPFC 590 > SPFC 440) under *t* = 1.8 mm and *Rp* = 6 mm and 3 mm. This effect is attributed to the low material strength, which reduces the influence of elastic recovery because of the decrease in material rigidity. However, the increasing rate of the springback angle of *Rp* = 6 mm is larger than that of *Rp* = 3 mm. The result also indicates that punch radius plays an important role in springback occurrence. Fig. 4(c) shows that the springback angle increases as punch radius increases under SPFC 440 and 590 and *t* = 1.4 mm and 1.8 mm. This effect is attributed to the small punch radius, which reduces the influence of elastic recovery because of the concentrated plastic zone in the bent part. In the cases of SPFC 440, the increase of the springback angle of *t* = 1.8 mm is limited. However, in the cases of *t* = 1.8 mm, the increase of the springback angle of SPFC 590 is larger than that of the springback angle of SPFC 440. Figs. 4(a)-(c) imply that a large sheet thickness value, low material strength, and small punch radius effectively reduce springback in vee bending.

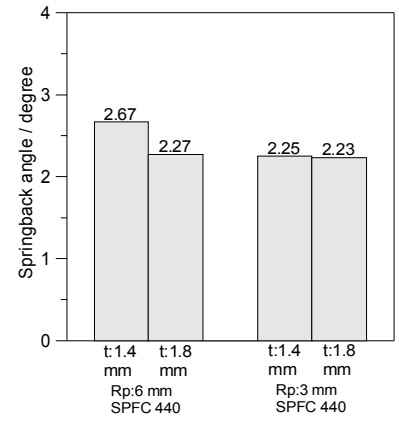

(a)

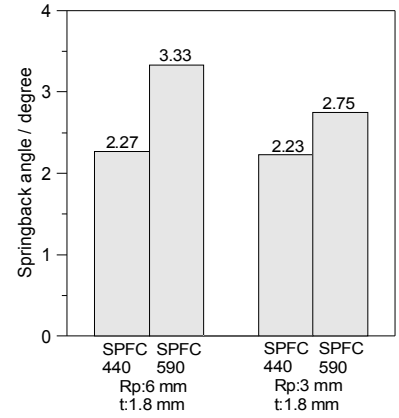

(b)

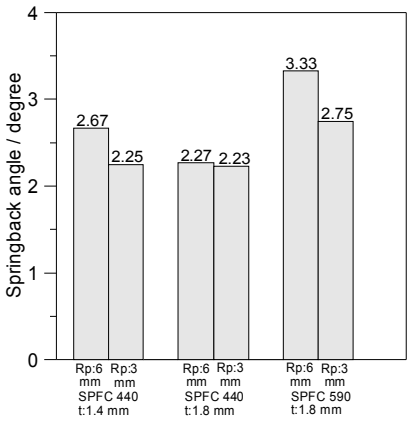

(c)

Fig. 4. (a) Effect of thickness on the springback angle under different punch radii; (b) effect of material strength on the springback angle under different punch radii; (c) effect of punch radius on the springback angle under different thickness and material strength values.

3.3 Effects of material properties on the springback ratio $(\Delta\theta/\theta)/(3K/E')$

In addition to experimentation, a numerical simulation based on Eq. (22) was performed to investigate the effects of the process parameters, namely, normal anisotropy *R*, the strain-hardening exponent *n*, and sheet thickness ratio $t/2\rho$, on the springback ratio $(\Delta\theta/\theta)/(3K/E')$ in the vee bending process, which are shown in Figs. 5(a)-(c). As shown in Fig. 5(a), the springback ratio decreases sharply with the thickness ratio at small *n* values. The slight decrease of the springback ratio with the thickness ratio is observed at large *n* values. Fig. 5(b) shows that the springback ratio increases nearly linearly with normal anisotropy *R*. Small thickness ratios and *n* values obviously result in a large springback ratio. Fig. 5(c) shows that the springback ratio decreases sharply as the *n* value increases at small thickness ratios. However, the springback ratio decreases slightly as the *n* value increases at large thickness ratios and is smaller than that at small thickness ratios. When the *n* value approaches unity, the springback

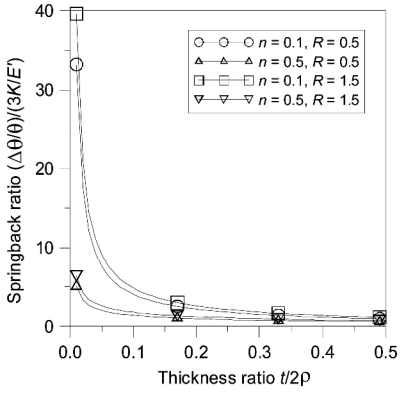

(a)

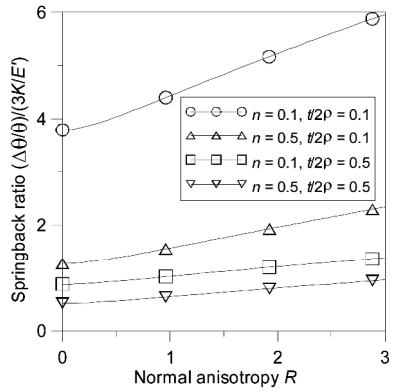

(b)

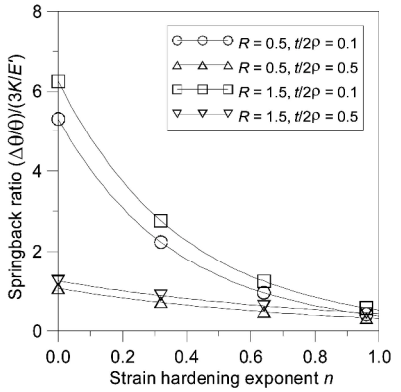

(c)

Fig. 5. (a) Effect of the thickness ratio on the springback ratio under different normal anisotropies and strain-hardening exponents; (b) effect of normal anisotropy on the springback ratio under different thickness ratios and strain-hardening exponents; (c) effect of the strain-hardening exponent on springback ratio under different thickness ratios and normal anisotropies.

ratio is concentrated within a small range, which is similar to the result shown in Fig. 5(a) in which the springback ratio is also concentrated within a decreasing range as the thickness ratio increases. The distributions of difference in Figs. 5(a)-(c) are similar to that in Ref. [8]; however, the proposed model is more precise than the model presented in Ref. [8], as shown in Table 2. From the aforementioned discussion, the following conclusions are drawn. (i) Springback is nearly proportional to normal anisotropy R. (ii) Springback decreases sharply with decreasing strain-hardening n values or thickness ratio $t/2\rho$ values. (iii) Springback is concentrated within a small range at large strain-hardening n values or large thickness ratio $t/2\rho$ values.

4. Conclusions

In this work, a simplified approach is developed by considering the thickness ratio, normal anisotropy, and the strain-hardening exponent to estimate the springback angle of vee bending based on elementary bending theory and the pure bending model. In addition, a series of experiments is performed to verify the proposed model and clarify the effects of punch radius, sheet thickness, and material strength on the springback angle. This study yielded the following findings.

(1) A consistent agreement is achieved in the comparison between the predicted values and the experimental results, which reflects the reliability of the proposed model. Furthermore, the present work is more accurate than previous works on springback prediction.

(2) In the developed model, the springback angle is directly proportional to the initial strain and inversely proportional to the modulus of elasticity within the elastic limit because of the linear relationship of elastic deformation.

(3) The analysis of the experimental results indicates that a large sheet thickness value, low material strength, and small punch radius effectively reduce the springback angle in vee bending.

(4) The numerical simulation shows that the springback ratio increases as normal anisotropy increases or as the thickness ratio and the strain-hardening exponent decrease.

This work can be used as a process design guideline to reduce the springback of HSS sheets in vee bending.

Acknowledgment

The authors would like to thank the Ministry of Science and Technology (National Science Council) of the Republic of China for financially supporting this research under Contract No. NSC 102-2815-C-149-004-E.

References

[1] F. J. Gardiner, The springback of metals, *ASME Journal of Applied Mechanics*, 79 (1957) 1-9.

[2] J. Datsko and C. T. Yang, Correlation of bendability of materials with their tensile properties, *ASME Journal of Engineering for Industry*, 82 (1960) 309-314.

[3] N. Takenaka, Y. Tozawa and K. Suzuki, Material characteristic value for evaluation of bendability and methods for measuring these values, *Ann CIRP*, 20 (1970) 53-54.

[4] V. Cupka, T. Nakagawa, H. Tiyamoto and H. Kudo, Fine bending with counter pressure, *Annual CIRP*, 22 (1973) 73-74.

[5] J. A. G. Kals and P. C. Veenstra, On the critical radius in sheet bending, *Annual CIRP*, 23 (1974) 55-56.
[6] H. Ogawa, A. Makinouchi, H. Takizawa and N. Mori, Development of an elasto-plastic FE code for accurate prediction of springback in sheet bending processes and its validation by experiments, *Advanced Technology of Plasticity, Proceeding of the Fourth International Conference on Technology of Plasticity* (1993) 1641-1646.
[7] C. Wang, G. Kinzel and T. Altan, Mathematical modeling of plane-strain bending of sheet and plate, *Journal of Materials Processing Technology*, 39 (1993) 279-304.
[8] D. K. Leu, A simplified approach for evaluation bendability and springback in plastic bending of anisotropic sheet metals, *Journal of Materials Processing Technology*, 66 (1997) 9-17.
[9] D. K. Leu, Effects of process variables on V-die bending process of steel sheet, *International Journal of Mechanical Sciences*, 40 (7) (1998) 631-650.
[10] Y. M. Huang, Finite element analysis on the V-die coining bend process of steel metal, *International Journal of Advanced Manufacturing Technology*, 34 (2007) 287-294.
[11] D. K. Leu and C. M. Hsieh, The influence of coining force on spring-back reduction in V-die bending process, *Journal of Materials Processing Technology*, 196 (2008) 230-235.
[12] M. Bakhshi-Jooybari, B. Rahmani, V. Daeezadeh and A. Gorji, The study of spring-back of CK67 steel sheet in V-die and U-die bending processes, *Materials & Design*, 30 (7) (2009) 2410-2419.
[13] R. Narayanasamy and P. Padmanabhan, Application of response surface methodology for predicting bend force during air bending process in interstitial free steel sheet, *International Journal of Advanced Manufacturing Technology*, 44 (2009) 38-48.
[14] H. Y. Yu, Variation of elastic modulus during plastic deformation and its influence on springback, *Materials & Design*, 30 (2009) 846-850.
[15] F. Ozturk, R. E. Ece, N. Polat and A. Koksal, Effect of warm temperature on springback compensation of titanium sheet, *Materials and Manufacturing Processes*, 23 (9) (2010) 1021-1024.
[16] S. Chatti and N. Hermi, The effect of non-linear recovery on springback prediction, *Computers & Structures*, 89 (13-14) (2011) 1367-1377.
[17] H. Baseri, M. Bakhshi-Jooybari and B. Rahmani, Modeling of spring-back in V-die bending process by using fuzzy learning back-propagation algorithm, *Expert Systems with Applications*, 38 (7) (2011) 8894-8900.
[18] C. C. Chen and C. P. Jiang, Grain size effect in the micro-V-bending process of thin metal sheets, *Materials and Manufacturing Processes*, 26 (1) (2011) 78-83.
[19] J. Y. Lee, J. W. Lee, M. G. Lee and F. Barlat, An application of homogeneous anisotropic hardening to springback prediction in pre-strained U-draw/bending, *International Journal of Solids and Structures*, 49 (25) (2012) 3562-3572.
[20] C. P. Jiang and C. C. Chen, Grain size effect on the springback behavior of the micro tube in the press bending process, *Materials and Manufacturing Processes*, 27 (5) (2012) 512-518.
[21] Z. M. Fu, Numerical simulation of springback in air-bending forming of sheet metal, *Applied Mechanics and Materials*, 121-126 (2012) 3602-3606.
[22] V. Malikov, R. Ossenbrink, B. Viehweger and V. Michailov, Experimental investigation and analytical calculation of the bending force for air bending of structured sheet metals, *Advanced Materials Research*, 418-420 (2012) 1294-1300.
[23] Y. Song and Z. Yu, Springback prediction in T-section beam bending process using neural networks and finite element method, *Archives of Civil and Mechanical Engineering*, 13 (2) (2013) 229-241.
[24] D. K. Leu, Position deviation in V-die bending process with asymmetric bend length, *International Journal of Advanced Manufacturing Technology*, 64 (2013) 93-103.
[25] K. J. Weinmann and R. J. Shippell, Effect of tool and workpiece geometries upon bending forces and springback in 90 degree V-die bending of HSLA steel plate, *Sixth North American Metal Working Research Conference Proceeding* (1978) 220-227.
[26] M. Ramezani, Z. Mohd Ripin and R. Ahmad, Modelling of kinetic friction in V-bending of ultra-high-strength steel sheets, *International Journal of Advanced Manufacturing Technology*, 46 (2010) 101-110.
[27] Z. Fu and J. Mo, Multiple-step incremental air-bending forming of high-strength sheet metal based on simulation analysis, *Materials and Manufacturing Processes*, 25 (8) (2010) 808-816.
[28] M. Ramezani and Z. Mohd Ripin, A friction model for dry contacts during metal-forming processes, *International Journal of Advanced Manufacturing Technology*, 51 (2010) 93-102.
[29] Z. Fu and J. Mo, Springback prediction of high-strength sheet metal under air bending forming and tool design based on GA-BPNN, *International Journal of Advanced Manufacturing Technology*, 53 (5-8) (2011) 473-483.
[30] N. Kardes Sever, O. H. Mete, Y. Demiralp, C. Choi and T. Altan, Springback prediction in bending of AHSS-DP 780, *Proceedings of North American Manufacturing Research Institute/ Society of Manufacturing Engineers*, 40 (2012) 1-10.
[31] D. K. Leu, Position deviation and springback in V-die bending process with asymmetric dies, *International Journal of Advanced Manufacturing Technology*, 79 (2015) 1095-1108.

Daw-Kwei Leu obtained his M.S. and Ph.D. in Mechanical Engineering from the National Taiwan University of Science and Technology in 1984 and 1995, respectively. Dr. Leu is currently a Professor at the Department of Mechanical Engineering, Taipei Chengshih University of Science and Technology, Taiwan. His main research fields are plasticity, metal forming processes, microforming and contact friction.